Coupled Substrate-Resonator-Electrostatic Simulation and Validation of High-Q MEMS Resonator Performance

Y. H. Park* and K. C. Park**

Department of Aerospace Engineering Sciences, University of Colorado, Boulder, CO, USA,
* yhpark@colorado.edu, ** kcpark@titan.colorado.edu

ABSTRACT

Vibration energy transmission from MEMS resonator through anchor to substrate, viz., anchor loss, is examined by utilizing the coupled substrate - resonator - electrostatic numerical model. The substrate and resonator beam are modeled independently and then integrated by enforcing their interface compatibility condition and the electrostatic force equilibrium to arrive at the multiphysics model. The present model has been validated with several reported sing-beam resonators. The validated model indicates that: the anchor loss is a frequency dependent mechanism that increase with increasing frequency, and the resulting equivalent damping coefficient due to anchor loss is 0.15 % for 71.8 MHz resonator; the resonant frequency of the beam decreases up to 5 % due to substrate flexibilities interacting with the beam at the anchors.

Keywords: MEMS resonator, Q-factor, Anchor loss.

1 INTRODUCTION

One of the promising applications of MEMS devices appears to be micro-resonators that act as IC-compatible components for communication systems. It is generally agreed that the two design challenges of these devices are high Q-factors and high operating frequency ranges from several mega to gega Hertz. For the particular class of resonators as shown in Figure 1, many of fabricated resonators exhibit that vibration energy transmission from MEMS resonator through anchor to substrate, viz., anchor loss is a crucial energy loss path limiting the achievement of high Q-factor as operating frequency increases up to HF to VHF ranges [1], [2].

In this study, for the ultimate goal of design improvement, the anchor loss mechanism is numerically modeled and validated by correlation with experiments of a series of clamped beam resonators whose center frequencies range from 8 MHz to 70 MHz. The modeling procedure is divided into two parts as illustrated in Figure 2: substrate model is generated analytically via a modified classical wave propagation solution, and a resonating beam plus electromechanical coupling is modeled with finite element method. To account for model uncertainties, adjustment parameters are allowed for the mass,

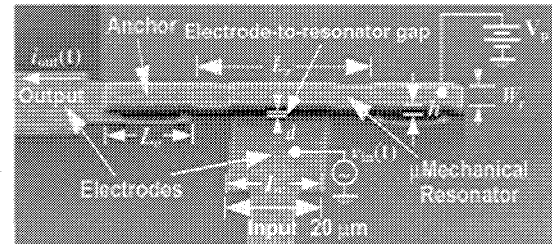

Figure 1: SEM of the clamped-clamped resonator beam and circuit connections (source: Bannon et al.[2]).

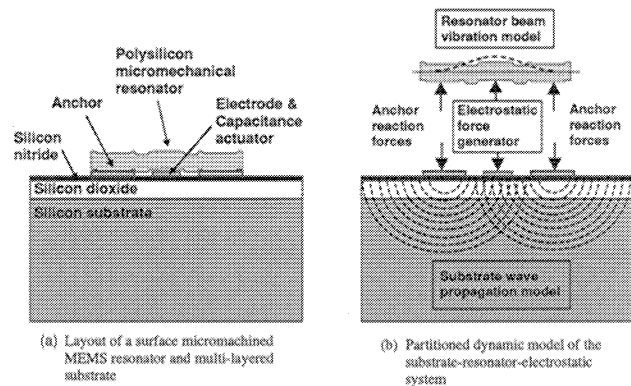

Figure 2: Typical clamped-clamped beam resonator actuated electrostatically in vertical direction to the substrate. Motion of the resonator generates anchor forces at both ends, in turn the vibration is radiated into the substrate as a wave motion.

stiffness, and damping matrices. Then independent two models are coupled by enforcing interface compatibility to arrive at the coupled dynamics model. Based on the verified numerical model, the resonator performance changes due to substrate effect such as Q-factor and center frequency changes are examined.

2 SUBSTRATE MODEL

In most surface micromachining processes, a typical substrate consists of silicon composite layers on the top surface plus silicon wafer as shown in Figure 2 [3]. To find the wave propagation due to anchor excitation, a harmonic force is applied on anchor pad and its re-

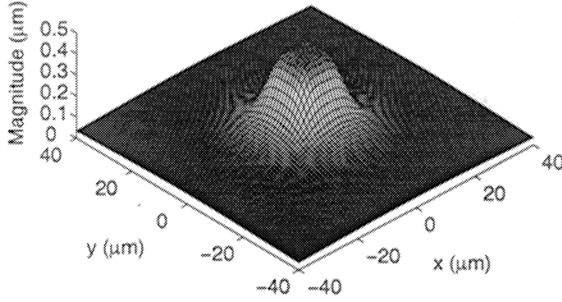

Figure 3: Substrate deformation: the magnitude of the vertical displacement with 1 μm-resolution around the anchor area at the top surface due to a unit vertical anchor excitation of 40 MHz.

sulting substrate response is computed for an exciting frequency, ω. The wave propagation in the substrate constitutes the well-known classical wave propagation problem in elastic half-space for which a variety of solution techniques have been developed over the years (see, e.g., [4]). In present study, we have chosen a semi-analytical approach using an inverse-Fourier transform method to solve the wave propagation so that the wave motion of the multilayered silicon substrate can be accounted for. Detailed solution procedure is shown in the preceding authors' work[5]. Figure 3 plots the resulting deformation of the substrate in the vicinity of the anchor area.

Having found the harmonic displacement due to the anchor excitation, we can develop the force-displacement relationship of the substrate using a receptance matrix $\mathbf{H}^s(\omega)$, which means physically the resulting harmonic displacement caused by a unit harmonic force as

$$\begin{bmatrix} \mathbf{H}^s_{EE}(\omega) & \mathbf{H}^s_{EA}(\omega) \\ \mathbf{H}^s_{AE}(\omega) & \mathbf{H}^s_{AA}(\omega) \end{bmatrix} \begin{Bmatrix} \mathbf{F}^s_E \\ \mathbf{F}^s_A \end{Bmatrix} = \begin{Bmatrix} \mathbf{X}^s_E \\ \mathbf{X}^s_A \end{Bmatrix} \qquad (1)$$

where superscript s denotes substrate; $\mathbf{H}^s(\omega) = [H^s_{ij}(\omega)]$ for $i, j = 1, 2, ..., n$; and, subscripts E and A indicate the electrode and the anchor nodes on the substrate, respectively. Once the substrate receptance is obtained, the identified substrate response characteristics is merged to the resonator beam model.

3 RESONATOR MODEL

A dynamic model of MEMS resonator beam is developed accounting for structural properties and electromechanical coupling effect by the finite element method. Figure 1 shows a surface micromachined resonator[2] which will be modeled. The finite element model of the resonator beam can be written in terms of its mass, damping, stiffness matrices, and the external forces as

$$\mathbf{M}\ddot{\mathbf{x}}(t) + \mathbf{C}\dot{\mathbf{x}}(t) + \mathbf{K}\mathbf{x}(t) = \mathbf{f}_A(t) + \mathbf{f}_E(t) \qquad (2)$$

where $\mathbf{f}_A$ is the reaction force vector acting on the anchors; $\mathbf{f}_E$ is the electrostatic force acting on the resonator beam; $\mathbf{x}(t)$ is the time-varying deformation of the beam; and, structural matrices $\mathbf{M}$, $\mathbf{C}$, and $\mathbf{K}$ are defined for the case when the anchors are detached from the substrate, so called, the free-free boundary case. This free-free resonator beam will then be coupled to the substrate. Assuming small deflection of the beam $x(t)$ ($|x(t)| \ll d$, where d is the electrode-to-resonator gap) and small input signal voltage $v_{in}(t)$ ($|v(t)_{in}| \ll V_p$, where V_p is the bias voltage), the electrostatic force in equation (2) can be obtained as

$$\mathbf{f}_E(t) = \mathbf{K}_E\mathbf{x}(t) + \mathbf{f}_v v_{in}(t) \qquad (3)$$

$$\mathbf{K}_E = [k_{Eii}] = [\varepsilon A_i V_p^2/d^3], \qquad (4)$$

$$\mathbf{f}_v = \{-\varepsilon A_i V_p/d^2\} \qquad \text{for i=1,2,...m.} \qquad (5)$$

where A_i is the area in the vicinity of the i-th electrode node; ε is the free space permittivity; $v_{in}(t)$ is the input signal voltage; $\mathbf{K}_E$ is called an *electric stiffness matrix* [2] having only m nonzero diagonal entries corresponding to the vertical displacement of the beam electrode nodes; and, $\mathbf{f}_v$ is called an *electromechanical coupling vector* which converts the input voltage to a mechanical force vector. Finally, the resulting output current from the beam electrode can be obtained using the electromechanical coupling vector as [2]

$$i_{out}(t) = \mathbf{f}_v^T \dot{\mathbf{x}}(t). \qquad (6)$$

By using the finite element model of the resonator beam in equation (2), the receptance model of the resonator beam can be expressed as

$$\begin{bmatrix} \mathbf{H}^b_{EE}(\omega) & \mathbf{H}^b_{EA}(\omega) \\ \mathbf{H}^b_{AE}(\omega) & \mathbf{H}^b_{AA}(\omega) \end{bmatrix} \begin{Bmatrix} \mathbf{F}^b_E \\ \mathbf{F}^b_A \end{Bmatrix} = \begin{Bmatrix} \mathbf{X}^b_E \\ \mathbf{X}^b_A \end{Bmatrix} \qquad (7)$$

where superscript b denotes resonator beam. The resonator receptance matrices in equation (7) can be constructed from the modal summation as [6]:

$$\mathbf{H}^b(\omega) = \sum_{n=1}^{N_b} \frac{\{\phi^b_n\}\{\phi^b_n\}^T}{\omega_n^2 - \omega^2 + 2i\zeta_n\omega_n\omega} \qquad (8)$$

where ω_n, ζ_n, and $\{\phi^b_n\}$ are the *n-th* natural frequency, modal damping ratio, and mass normalized mode shape of the resonator beam, and N_b is the number of dominant modes chosen. All the modal properties in equation (8) can be obtained from the modal analysis of the beam finite element model, i.e., by solving the eigenvalue problem when the resonator beam is freely vibrating without all the mechanical and electromechanical external forcing terms on the right hand side of equation (2).

Table 1: Summary of simulation results (Sim.) and comparison with experiment (Exp.).

Parameter	case 1 [2]	case 2 [7]	case 3 [1]	case 4 [1]
Resonator length, L_r (μm)	40.8	30	16	14
Center frequency, f_c (Exp./Sim., MHz)	8.51 / 8.51	15.4 / 15.4	54.2 / 54.2	71.8 / 71.8
Q-factor, Q_{res} (Exp./Sim.)	8000 / 8326	1600 / 2544	800 / 880	300 / 306
Q-factor with rigid substrate, Q_{ideal} (Sim.)	8624	7628	7867	8330
Damping ratio, ζ_{res} (Exp./Sim., $\times 10^{-4}$)	0.63 / 0.60	3.13 / 1.97	6.25 / 5.68	16.67 / 16.34
• material damping contribution, ζ_{mat}	0.58 (97%)	0.66 (34%)	0.64 (11%)	0.60 (4%)
• anchor loss contribution, ζ_{al}	0.02 (3%)	1.31 (66%)	5.04 (89%)	15.74 (96%)

4 COUPLED TRANSFER FUNCTION

The interface condition at the anchor nodal points can be described by the kinematic compatibility and the force equilibrium at the anchor nodes. In addition, we have an equilibrium condition of electrostatic force between the electrodes of the substrate and the resonator beam as follows:

$$\text{anchor kinematic compatibility: } \mathbf{X}_A^b - \mathbf{X}_A^s = \mathbf{0}; \quad (9)$$

$$\text{anchor force equilibrium: } \mathbf{F}_A^b + \mathbf{F}_A^s = \mathbf{0}; \quad (10)$$

$$\text{electrode force equilibrium: } \mathbf{F}_E^b + \mathbf{F}_E^s = \mathbf{0}. \quad (11)$$

Substituting the above interface conditions into the uncoupled receptance equation (1) of the substrate and equation (7) of the resonator beam, we can get the mechanical receptances of the coupled substrate-resonator system. As a result of mathematical derivations using the coupled receptance and the electro-mechanical coupling equation (3), the voltage-current transfer function is obtained as

$$I_{out} = g_{iv}(\omega) V_{in}, \qquad i_{out}(t) = I_{out} e^{i\omega t} \quad (12)$$

$$\begin{aligned} &\text{where } g_{iv} = i\omega\, \mathbf{f}_v^T \mathbf{G}_{xv}(\omega)\, \mathbf{f}_v \\ &\mathbf{G}_{xv}(\omega) = [\mathbf{I} - \tilde{H}_{EE}^b(\omega)\, \mathbf{K}_E]^{-1} \tilde{H}_{EE}^b(\omega)\, \mathbf{f}_v \\ &\tilde{H}_{EE}^b(\omega) = \mathbf{H}_{EE}^b(\omega) - \mathbf{H}_{EA}^b(\omega)\, \tilde{B}_{AE}(\omega) \\ &\tilde{B}_{AE}(\omega) = -[\mathbf{H}_{AA}^b + \mathbf{H}_{AA}^s]^{-1}[\mathbf{H}_{AE}^b + \mathbf{H}_{AE}^s] \end{aligned} \quad (13)$$

The detailed derivations are shown in the preceding authors' work[5]. The output signal voltage $v_{out}(t)$ is measured using a proper amplification of the output current, e.g., using a transresistive amplifier in reference [2]. The transmissibility of the signal voltage is

$$Transmissibility(dB) \equiv 20\log(\tfrac{|V_{out}|}{|V_{in}|}) \quad (14)$$

$$\text{where} \qquad v_{out}(t) = V_{out} e^{i\omega t} \quad (15)$$

Note that the transfer function in equation (12) can be evaluated using the mechanical receptances obtained from the separate analyses of the resonator beam and the substrate along with the electromechanical coupling matrices in equation (3).

5 SIMULATION AND DISCUSSION

The present coupled substrate-resonator model is validated by correlating with the published experimental data for a series of clamped-clamped beam μ-resonators. Four different designs of μ-resonators which have center frequencies from 8.51 MHz to 71.8 MHz have been used to investigate the anchor loss effect. Table 1 summarizes the published resonator specifications and experimental data[1], [2], [7]. Figure 4 shows the layout of the resonator beam FE model consisting of a free-free beam and two anchor blocks which connect the beam to the substrate. To capture the general 3-dimensional motion of each node, SOLID45 8-node brick element of ANSYS 5.7 is utilized. In general, a finite element model has parametric uncertainties in mass, stiffness and damping, which come in large part from manufacturing tolerance, residual stress due to thermal expansion, irregular surface topography, chemical contamination, and material property variations, among others. To account for the uncertainties of the finite element model, we introduce adjustment parameters m, k and γ as

$$\mathbf{M} = m\mathbf{M}_o, \;\; \mathbf{K} = k\mathbf{K}_o, \mathbf{C} = \gamma\mathbf{K}/\omega \quad (16)$$

where $\mathbf{M}_o$ and $\mathbf{K}_o$ are the initial mass and stiffness matrices, respectively; γ is the damping adjustment parameter that accounts for the stiffness-proportional material damping of the resonator beam [6]. From the experimental observations of the existing free-free beam resonators with Q-factors of around 8,000 under vacuum condition, the stiffness proportional damping parameter γ of polysilicon is found approximately as [5]

$$\gamma = 1/Q_n \approx 1.25 \times 10^{-4} \quad (17)$$

The parameters m and k are adjusted in order for each resonator simulation model to have the same center frequency, maximum deformation as those of each experiment in references[1], [2], [7].

Figure 5 shows the experimental and the simulated transmissibility curves of case 3 resonator with the center frequency of 54.2 MHz [1]. The simulation matches well with the experiment: the experimental Q-factor is

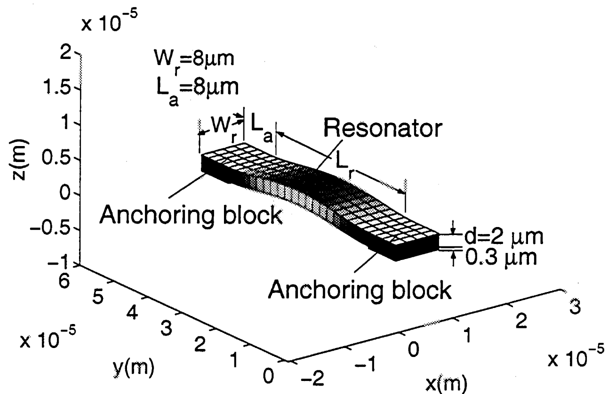

Figure 4: Geometry and FE model of the resonator beam.

840 and that of the simulation is 880. The effect of the substrate flexibility for case 3 is severe compared with the case 1 as shown in Table 1: the center frequency decreases by 1.37 MHz (2.3 %) from that of rigid substrate case. As shown in Table 1, the Q-factor decreases by about 89 % from the ideal case (from 7867 to 880) primarily due to its anchor loss. Table 1 summarizes the center frequencies; the Q-factors of the experiments (Q_{res}) and of the ideal rigid substrate cases (Q_{ideal}); and, the damping ratios of the simulations and the experiments for each correlation case.

Based on the validated numerical model, the contribution of anchor loss ζ_{al} to the damping ratios of the coupled substrate-resonator ζ_{res} is identified from the following expression

$$\zeta_{res} = 1/2Q_{res} = \zeta_{mat} + \zeta_{al} \tag{18}$$

where Q_{res} denotes the verified Q-factor of the resonator and ζ_{mat} is the identified material damping ratio. Table 1 summarizes the damping ratio ζ_{al} for each case. As the center frequency increases, the total damping ratio increases exponentially, due largely to anchor loss. For example, in the case of the 71.8 MHz resonator, the damping caused by the anchor loss is 15.7×10^{-4} whereas that caused by the material damping is only 0.6×10^{-4}.

6 CONCLUSIONS

A coupled electromechanical model of a clamped-clamped μ-resonator beam and multilayered substrate has been developed for the assessment of anchor loss. Since each of the component models are independent and modular, design changes can be easily implemented into the coupled model. Therefore, simulations for design modifications and remodeling can be expedited.

The correlation analysis with experiments has revealed that the material damping remains almost con-

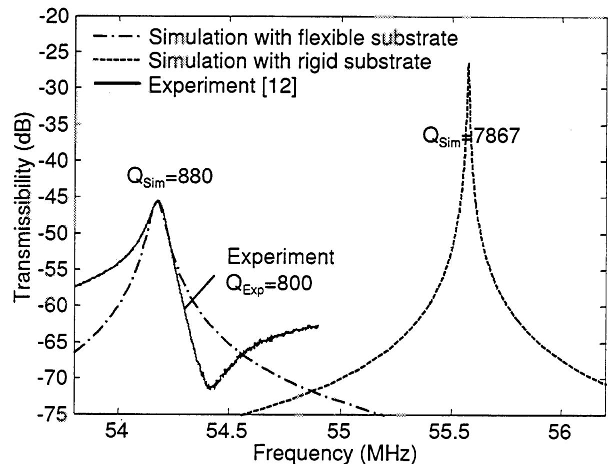

Figure 5: Transmissibility of a 54.2 MHz resonator [1] with the flexible and the rigid substrate.

stant for a wide range of operating frequencies, e.g., with the damping ratio about 0.006 % for polysilicon beam-type resonators. The frequency-dependent energy loss mechanism is found to be primarily responsible for anchor loss, whose damping ratio is identified to be 0.15% for a 71.8 MHz resonator. In addition, it is found that decrease in the center frequency from the theoretical value of the resonator beams is partially due to the substrate flexibilities at the anchor points. As the center frequency increases, so does the frequency drop, e.g., 5.3% drop for a 71.8 MHz resonator.

REFERENCES

[1] K. Wang, Y. Yu, A.-C. Wong, and C. T.-C. Nguyen, '*Technical Digest, 12th International IEEE Micro Electro Mechanical Systems Conference*, Orlando, Florida, Jan. 17-21, 453-458,1999.

[2] F. D.Bannon III, J. R. Clark, and C. T.-C. Nguyen, *IEEE J. of Solid State Circuits*, Vol. 35, No. 4, 512-526, 2000.

[3] C. T.-C. Nguyen and R. T. Howe, *IEEE J. of Solid State Circuits*, Vol. 34, No. 4, 512-526, 1999.

[4] D. V. Jones, D. Le Houedec, and M. Petyt, *Journal of Sound and Vibration*, Vol. 212, No. 1, 61-74, 1998.

[5] Y. H. Park and K. C. Park, "High-Fidelity Modeling of MEMS Resonators - Part I and II," submitted to *Journal of Microelectromechanical System*, 2002.

[6] D. J. Ewins, "Modal Testing: Theory and Practice", John Wiley & Sons Inc., 45-48, 1984.

[7] J. R. Clark, A.-C. Wong, and C. T.-C. Nguyen, *Digest of Technical Papers, 1997 International Conference on Solid-State Sensors and Actuators*, Chicago, Illinois, June 16-19, 1161-1164, 1997.